Vol. 90: 59–76, 2023
https://doi.org/10.3354/cr01714

CLIMATE RESEARCH
Clim Res

Published July 6 §

Contribution to CR Special 36 'Observed changes in climate over Asia'

Extreme precipitation changes over the Yangtze River Basin in 1901–2020

Siqi Zhang[1,2], Guoyu Ren[1,2,*], Yunjian Zhan[3], Cunjie Zhang[1], Yuyu Ren[1]

[1]National Climate Center, China Meteorological Administration (CMA), Beijing 100081, PR China
[2]Department of Atmospheric Science, School of Environmental Studies, China University of Geosciences (CUG), Wuhan 430074, PR China
[3]National Meteorological Information Center, China Meteorological Administration, Beijing 100081, PR China

ABSTRACT: To better understand the characteristics of long-term change and variability in regional extreme precipitation and to examine possible regional responses to global climate warming, we analyzed temporal and spatial patterns of precipitation and extreme precipitation index changes in the Yangtze River Basin (YRB) over the last 120 yr. Based on the China Meteorological Administration's daily precipitation data set of 60 city stations in mainland China from 1901–2020, we found that total annual precipitation and daily precipitation intensity of the Upper Reaches (UR) experienced a downward trend, but those of the Middle and Lower Reaches (MLR) showed an upward trend. Precipitation amount and intensity increased, while the number of precipitation days slightly decreased over the YRB during 1901–2020. Most extreme precipitation indices showed a decreasing trend in the first 60 yr that reversed after 1961 into slightly upward trends, except for consecutive dry days and wet days in the YRB during 1901–2020. There were significant downward trends for consecutive dry days and maximum 1 and 5 d precipitation during the first 60 yr, and significant upward trends for maximum 1 d precipitation, total extreme heavy precipitation, and very heavy precipitation days in the last 60 yr. The trends for extreme precipitation in the UR were lower than those in the MLR during 1901–2020, particularly in the last 60 yr, whereas the trends in the UR were higher than those in the MLR during 1901–1960. The fluctuations of extreme precipitation indices in the UR were more dramatic than those in the MLR, and the extreme precipitation indices all showed 5–10 or 20 yr periodic variabilities. The analysis also showed that observed changes in regional extreme events were directly related to rapid urbanization around the stations and multi-decadal variability of the East Asian monsoon.

KEY WORDS: Precipitation · Extreme precipitation · Trend · Yangtze River Basin · The last 120 years

1. INTRODUCTION

Global warming has led to significant changes in the intensity, frequency, seasonality, and spatial distribution of climate variables, including temperature, humidity, wind, and snow (IPCC 2021). Global and regional extreme precipitation has received significant attention and has become a crucial metric for monitoring and studying climate change (Zhai et al. 2005, 2007, Min & Qian 2008, Tu et al. 2010, Ren et al. 2011, 2015, Donat et al. 2013, 2016, Westra et al. 2013, Han et al. 2019, IPCC 2021).

The Yangtze River Basin (YRB) is China's paramount climate-response region, where the frequency of extreme precipitation and disasters caused by floods is higher than in other regions. Numerous studies have investigated extreme precipitation events in the YRB (J. M. Chen et al. 2014, Pan et al. 2017). Total precipitation in the Basin, especially in the middle and lower reaches (MLR), has signif-

*Corresponding author: guoyoo@cma.gov.cn

§ Article was changed to Open Access, and the copyright notice updated after publication.
This corrected version: August 31, 2023

Publisher: Inter-Research · www.int-res.com

icantly increased in the last few decades (Yang et al. 2005, Huang et al. 2006, He et al. 2013), which is the main reason for the increasing intensity of precipitation events, especially in recent years (Feng et al. 2011, Fu et al. 2013, He et al. 2013, Ren et al. 2015, Zhang et al. 2020). Additionally, most of the extreme precipitation indices show significant upward trends, with the most remarkable high-value areas located in Jiangxi, southeastern Hubei, and northeast Hunan provinces (Su et al. 2006, Wang et al. 2008, Wu et al. 2016).

When showing increasing trends over recent decades in the MLR, most of the indices exhibit periodic oscillations of 12–16 yr or longer (Wang et al. 2008, Ren et al. 2011, Zhang & Ma 2011). Although precipitation tends to be extreme as a whole in the YRB, it is not known if the recent trends are components of low-frequency variabilities. In order to better understand whether the change observed is a half-cycle feature in the periodic fluctuations of multi-decadal to century scales, there is a need to collect and analyze century-long records of precipitation data. Such an analysis is important for not only the detection and attribution of regional total and extreme precipitation change, but also for the development of decadal precipitation prediction techniques in the YRB.

For precipitation change at the 100 yr scale in the YRB, Jian et al. (1986) used the regression reduction method and ratio method to extend monthly precipitation data from 9 stations, and Zhang (1993) estimated the inter-decade variability of precipitation over the MLR in the 20th century. Li et al. (2012) collected and processed China's nationwide monthly station observational precipitation data from 1901–2010; the data were tested for homogeneity, and the inhomogeneous part of the series was adjusted. According to Jian et al. (1986) and Li et al. (2012), precipitation in the YRB has shown upward trends and periodic oscillations, especially in the MLR; Zhan et al. (2018) verified this finding. However, the time periods of the aforementioned studies on the characteristics of extreme precipitation changes only encompass several recent decades (1961–2020) and lack attention to the 100 yr scale in the YRB. This is because the previously used data sets did not include daily precipitation data prior to 1951 (Ren et al. 2012, Jaffrés 2019).

Although reanalysis and climate model data sets are important sources for analyzing precipitation and extreme precipitation values at the 100 yr scale, these reanalyses have the problem of incorporating errors from the assimilation processes, prediction models, and observation systems (Bengtsson et al. 2004, Zhao et al. 2010, 2015, Zhou et al. 2018, Zhang et al. 2019, 2021). The climate model data sets need to be verified and evaluated due to the complexity of the global climate system, the representativeness and reliability of climate models, and the ability of global climate models to simulate climate change (Song & Zhou 2014, Xu & Xu 2012, X. C. Chen et al. 2014, Pendergrass & Hartmann 2014, Akinsanola et al. 2020). In addition, the characteristics of the long-term changes and variability in regional extreme precipitation are currently not clear, and there are questions about the regional response of extreme precipitation to global climate warming. Hence, it was necessary to analyze a daily precipitation data set at a 100 yr scale to assess the change in extreme precipitation.

Zhan et al. (2022) developed a new data set that used the daily precipitation data of 60 cities in China from the National Meteorological Information Center, China Meteorological Administration (CMA). This data set, which was subjected to strict quality control, data interpolation, and splicing in the early 20th century, is considered the most suitable observation data for use in extreme precipitation change studies at the 100 yr scale in China. However, owing to instrumentation changes, station relocations, and different periods of observations, the daily precipitation inhomogeneity of a few observational stations may lead to uncertainties in the study of trends during the 20th century (Alexandersson 1986, Liu & Sun 1995, Dai et al. 1997, Wu 2005, Li et al. 2008, Wang et al. 2012, Yang & Li 2014).

In this study, we analyzed extreme precipitation in the YRB, extending the precipitation time series back to 1901, with an objective to better understand the total and extreme precipitation changes, including inter-decadal, multi-decadal, and century-scale variabilities, and the possible association between regional extreme precipitation and global climate warming. Our analysis also makes up for the paucity of research stemming from a lack of observational data in the first half of the 20th century.

2. DATA AND METHODS

2.1. Data selection and station information

We selected 17 national weather stations in the YRB from the daily precipitation data set of 60 city stations in mainland China from 1901–2020, which has been

strictly quality-controlled and interpolated (Zhan et al. 2022). This data set incorporated multiple sources of digital daily precipitation data before 1951 to supplement the previously missing and erroneous data, and then combined the modern daily precipitation data from 1951 onward. Data processing, which included metadata information supplementation, unit consistency check, quality control, and data merging, was implemented based on multiple sources of digitized daily precipitation data from 1901–1950. In addition, the data set was supplemented with previously unrecorded 'no precipitation' and missing data. A quality control schedule was developed, and quality control measures (including threshold values, extreme values, time consistency, and internal consistency checks) were carried out, some missing and erroneous data were filled in, and the early period data was combined with modern (since 1951) daily precipitation data.

The data set of daily precipitation was thus established for the past 120 yr (1901–2020) from 60 city stations in mainland China; 17 of those stations were in the YRB (which accounts for about 18.75% of the Chinese mainland). Among the 17 stations, 7 had valid records for >100 yr. Additionally, 6 of the stations were located in the Upper Reaches (UR) of the Yangtze River and 11 were located in the MLR (red and blue circles, respectively, in Fig. 1a). Fig. 1 and Table 1 show the distribution and information obtained from the 17 stations in the YRB from 1901–2020.

2.2. Precipitation and extreme precipitation index definition

In this study, the precipitation values for 4 annual total precipitation metrics and 8 extreme precipitation indices were calculated. The annual total precipitation metrics include precipitation amount (PREA), precipitation days (PRED), precipitation intensity (PREI), and precipitation frequency (PREF). PREA is defined as the sum of precipitation in the PRED, PRED is defined as the number of days with daily precipitation of >1 mm, PREI is defined as the ratio of PREA to PRED, and PREF is defined as the ratio of each grade of PRED to total PRED. The extreme precipitation index refers to the Expert Group on Climate Change Detection and Indicators website's index definition (Alexander et al. 2006, Klein Tank et al. 2009, Zhang et al. 2011): maximum 1 d precipitation (Rx1day), maximum 5 d precipitation (Rx5day), total heavy precipitation (R95p), total extreme heavy precipitation (R99p), heavy PRED (R20mm), very heavy PRED (R50mm), consecutive dry days (CDD), and consecutive wet days (CWD). These indices are listed in Table 2.

2.3. Statistical methods

In this study, we selected 1901–2020 as the research period. Based on the integrity of the data from 17 stations, we divided the 120 yr data set into 3 periods: 1901–1960, 1961–2020, and 1901–2020. The anomaly time series of extreme precipitation indices was calculated, and the climate reference period was 30 yr (1981–2010) because of the high data integrity during this period. Additionally, we used the area-weighted regional average method, which uses the cosines of the mid-grid latitudes as weights, to calculate the regional averages of all the indices and variables across the YRB.

The temporal features — in particular, the linear trend and inter-decadal variability — of the precip-

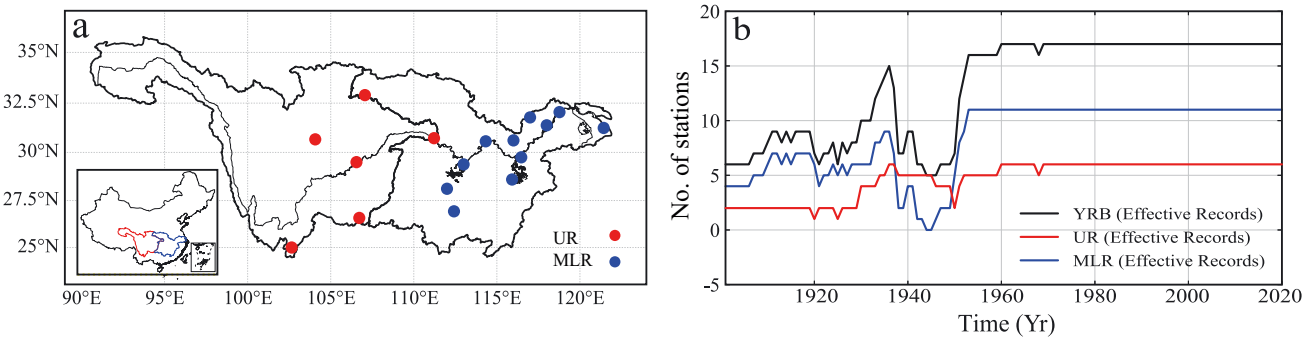

Fig. 1 (a) Yangtze River Basin (YRB), showing the distribution of the 17 national weather stations used in this study. Red dots: stations in the Upper Reaches (UR) of the YRB; blue dots: Middle and Lower Reaches (MLR). (b) Number of stations with effective records (stations including missing data that can be used to calculate the annual extreme index). Black line: total number of stations with effective records across the YRB; red and blue lines: number of stations with effective records in the UR and MLR, respectively

Table 1. Summary of the 17 national weather stations in the Yangtze River Basin (1901–2020). UR: upper reaches; MLR: middle and lower reaches

Yangtze River Basin				
Station	Latitude (° N)	Longitude (° E)	Years without data	Area
56778	25.00	102.65	1901–1929	UR
56290	30.67	104.07	1901–1933, 1950–1959	UR
57516	29.50	106.55	1920,1925	UR
57816	26.58	106.72	1901–1929, 1950	UR
57127	33.08	107.06	1901–1935, 1946–1950, 1968	UR
57461	30.73	111.22	1938–1951	UR
57584	29.38	113.08	1901–1909, 1921–1922, 1938–1952	MLR
57493	30.57	114.33	1921, 1929–1934, 1938–1947	MLR
58606	28.60	115.91	1901–1935, 1938–1950	MLR
58512	29.75	116.47	1915, 1925, 1938–1940, 1942–1950	MLR
58424	30.61	116.96	1901–1931, 1937–1938, 1942–1950	MLR
58321	31.78	117.30	1901–1945, 1949–1951	MLR
58334	31.38	118.36	1927–1928, 1932, 1936–1951	MLR
58238	32.05	118.77	1901–1906, 1913, 1920–1927, 1937–1948	MLR
58367	31.25	121.43	1942–1949	MLR
57871	26.93	112.78	1901–1932, 1939, 1944–1949	MLR
57679	28.11	113.08	1901–1910, 1923, 1938–1939, 1941–1946, 1979	MLR

Table 2. Definition of precipitation and extreme precipitation indices

Values	Name	Definition	Units
PREA	Precipitation amount	Sum of precipitation in precipitation days	mm
PRED	Precipitation days	Number of days with daily precipitation ≥1 mm	day
PREI	Precipitation intensity	Ratio of precipitation amount to precipitation days	mm d^{-1}
PREF	Precipitation frequency	Ratio of each grade of precipitation days to total precipitation days	%
Rx1day	Maximum 1 d precipitation	Highest precipitation amount in a 1 d period	mm
Rx5day	Maximum 5 d precipitation	Highest precipitation amount in a 5 d period	mm
R95p	Intense precipitation	Precipitation due to very wet days (>95th percentile)	mm
R99p	Extreme intense precipitation	Precipitation due to extremely wet days (>99th percentile)	mm
R20mm	Heavy precipitation days	Count of days where daily precipitation amount ≥20 mm	day
R50mm	Rainstorm days	Count of days where precipitation ≥ 50 mm	day
CDD	Consecutive dry days	Maximum length of dry spell (precipitation < 1 mm)	day
CWD	Consecutive wet days	Maximum length of wet spell (precipitation ≥ 1 mm)	day

itation values and extreme precipitation indices were analyzed. The linear trend (Tr) is the regression coefficient obtained using the least-squares method, as shown in Eq. (1), where P represents precipitation factor variables, t represents years, and n represents the number of each variable. The significance of the climate trend (S) represents the quantitative degree of the rise and fall in precipitation values and indices under climate change, as shown in Eq. (2):

$$Tr = \frac{\sum_{i=1}^{n} P_i t_i - \frac{1}{n}\left(\sum_{i=1}^{n} P_i\right)\left(\sum_{i=1}^{n} t_i\right)}{\sum_{i=1}^{n} t_i^{\,2} - \frac{1}{n}\left(\sum_{i=1}^{n} t_i\right)^2} \quad (1)$$

$$S = \frac{\sum_{i=1}^{n}\left(P_i - \overline{P}\right)\left(t_i - \overline{t}\right)}{\sqrt{\sum_{i=1}^{n}\left(P_i - \overline{P}\right)^2}\sqrt{\sum_{i=1}^{n}\left(t_i - \overline{t}\right)^2}} \quad (2)$$

To eliminate the influence of a linear trend, we eliminated the time-series trends of the extreme precipitation indices when examining inter-annual variability and periodic characteristics. We analyzed the inter-decade variability by averaging the extreme precipitation indices for every decade. Additionally, we used a wavelet to analyze the periodic characteristics of the time series, as shown in Eqs. (3) and (4):

$$Wf(a,b) = |a|^{-\frac{1}{2}} \int f(t)\,\overline{\psi}\left(\frac{t-b}{a}\right) dt \quad (3)$$

$$(1-t)=(1-t^2)\frac{1}{\sqrt{2\pi}}e^{-\frac{t^2}{2}}\ (-\infty<t<\infty) \quad (4)$$

where $Wf(a,b)$ is the wavelet transform coefficient, a is the frequency parameter used to determine the width of the wavelet, and b is the time parameter used to reflect the displacement of the wavelet. This study uses the Mexican hat wavelet in Eq. (3) to determine the frequency of a and the object of study sequence $f(t)$, and the mother wavelet function $\psi(t)$ in Eq. (4) to calculate the wavelet transform (Wei 2007).

3. RESULTS

3.1. Changes in precipitation values

The time series and box plots of anomalies for annual precipitation values (PREA, PRED, and PREI) over the YRB from 1901–2020 are shown in Fig. 2. In the early 20th century, PREA rapidly increased, followed by a downward trend from 1910–1930 and a trough in 1945. An upward trend in PREA occurred from 1940–1955, forming an obvious peak. From 1961–2020, PREA fluctuated with alternating high and low values. The highest PREA occurred in 1954 followed by 1912; the lowest was in 1978. The inter-decadal variability of PREA formed a trough in the 1920s and 1940s and a peak in the 1910s, 1950s, and 2010s. Abnormal PREA values mostly occurred in the 1910s and 1980s (Fig. 2a). The highest PRED occurred in 1912 followed by 1954. The inter-decadal variability of PRED was similar to that of PREA. The abnormally low values of PRED mostly occurred during the 1920s and 1940s, 1980–1990s and the 2010s. Abnormally high values occurred in the 1910s and 1950s (Fig. 2b). PREI exhibited a downward trend from 1900–1940, and thereafter showed a rising trend after 1950. Except for the 1940s, 1970s, and 2000–2010s, abnormally high PREI values mostly occurred during each decade (Fig. 2c).

Fig. 3 shows the time series and box plots of anomalies in annual precipitation values (PREA, PRED, and PREI) in the UR and MLR over the YRB during 1901–2020. The upward trend in PREA in the UR was higher than that in the MLR in the early 20th century. A downward trend was present from 1910–1930 and a trough occurred in 1942. Thereafter, PREA in the MLR increased gradually after 1970. The inter-decadal variability in PREA showed that the trough in the MLR was lower than that in the UR before the 1970s. Abnormal values of PREA mostly occurred during the 1900s–1930s, 1950s, and 1970s–2010s (Fig. 3a). PRED in the UR rapidly increased in the 1900s and slowly decreased during 1910–1920 before experiencing a trough in the 1940s. A weak upward trend in PRED in the MLR

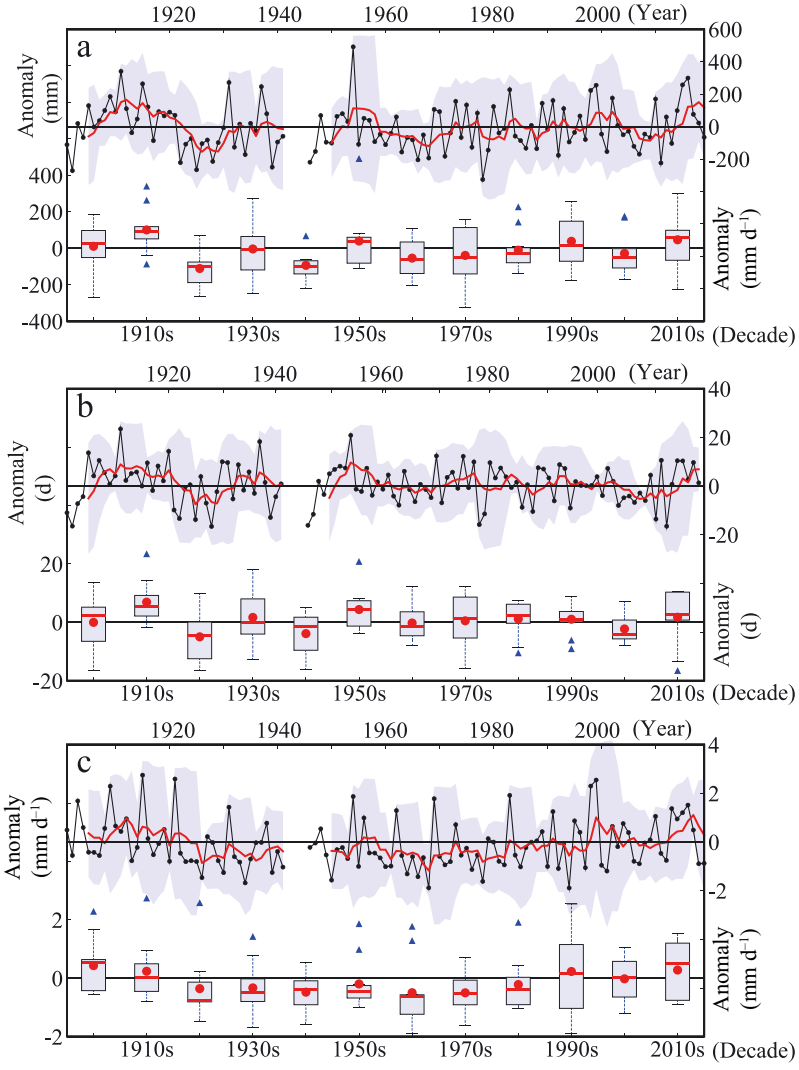

Fig. 2. Time series and box plots of anomalies in the precipitation values (a) precipitation amount (PREA), (b) precipitation days (PRED), and (c) precipitation intensity (PREI) over the Yangtze River Basin during 1901–2020. Red lines: 5 yr moving average; shading: the range of the 5 yr moving average ± the 5 yr moving SD. The dots, lines, and triangles in box plots represent the average of the anomaly, the median of the anomaly, and the abnormal values in every decade, respectively. The top and bottom of the box and the whiskers represent maximum, minimum, and the upper and lower quartiles, respectively

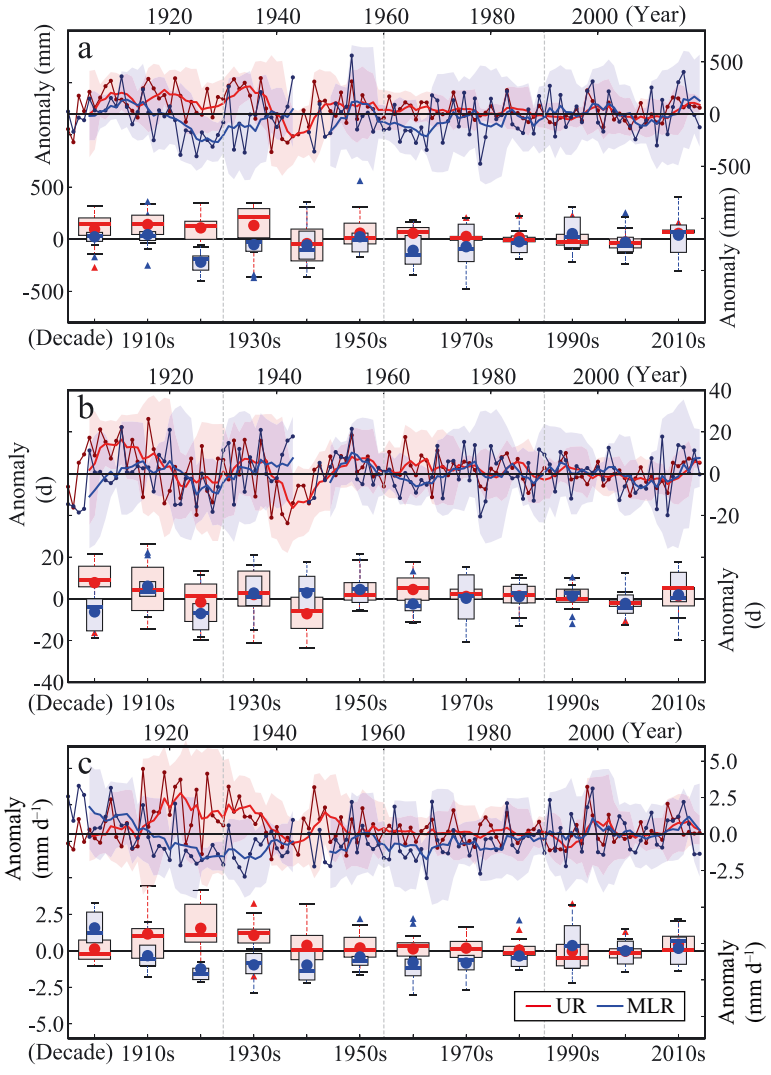

Fig. 3. Time series and box plots of anomalies for the precipitation values (a) precipitation amount (PREA), (b) precipitation days (PRED), and (c) precipitation intensity (PREI) over the Upper Reaches (UR), and Middle and Lower Reaches (MLR) of the Yangtze River Basin during 1901–2020. Red and blue lines: 5 yr moving average; shading: the range of the 5 yr moving average ± the 5 yr moving SD. Boxplot parameters as in Fig. 2

occurred during 1900–2020 and fluctuated with alternating high and low values. The inter-decadal variability of PRED matched that of PREA. The abnormal values of PRED mostly occurred in the first 20 yr and the last 30 yr (Fig. 3b). PREI in the UR slowly increased during the early 20th century before fluctuating with alternating high and low values. PREI in the MLR showed a remarkable downward trend during 1900–1940, followed by a rising trend after 1950. The inter-decadal variability in PREI formed a trough in the 1930s in the MLR and a peak in the 1900s and 2010s. The number of abnormally high values for PREI exceeded the number of abnormally low values (Fig. 3c).

Fig. 4 shows the daily PREA and PREF distributions over the YRB, the UR, and the MLR during 1901–1960 and 1961–2020. From 1901–1960, the daily PREA was concentrated between 1 and 10 mm and then decreased with the increasing precipitation categories in the YRB. PREF was concentrated between 1 and 10 mm and non-precipitation categories. From 1961–2020, PREA was concentrated between 1 and 25 mm and was higher than that in 1901–1961, whereas the PREA over 25 mm was lower than that in 1901–1961. In the most recent 60 yr, the frequency of days with no precipitation decreased while the frequency of days with PREAs between 1 and 10 mm increased. PREA and PREF concentrated between 1 and 10 mm in the UR was higher than that in the MLR.

Fig. 5 shows the periodic characteristic of precipitation values (PREA, PRED, and PREI) over the YRB, UR, and MLR during 1901–2020. PREA in the YRB had a 20 yr significant periodic characteristic during 1920–1960, and the wavelet power in the YRB was approximately 90 000. PREA in the YRB had a weak 2.5–5 yr periodic characteristic in the 1950s and 2000s. The powers of the PREA in the UR and MLR were higher than that in the YRB (Fig. 5a). The PRED had a slight 2.5–5 yr periodic characteristic in the 1930s–1940s and 1970s. A significant 20 yr periodic characteristic occurred during 1920–1960. The wavelet power for the 20 yr periodic characteristic of the PRED in the YRB reached 350. The power in the YRB for the 20 yr periodic characteristic was higher than that in the UR and MLR. Additionally, the indices in the MLR for the 5 yr periodic characteristic were higher than that in the YRB and UR (Fig. 5b). The PREI had a slight 2.5 yr periodic characteristic in the 1950s and a significant 2.5–5 yr periodic characteristic in the 1920s and 2000s. The powers in the MLR were greater than that in the UR and YRB (Fig. 5c).

Fig. 6 shows the linear trends in precipitation values (PREA, PRED, and PREI) over the YRB, UR, and MLR during 1901–1960, 1961–2020, and 1901–2020. The linear trends in PREA were not significant over the last 120 yr, except in the UR. Most of the stations decreased weakly before 1961,

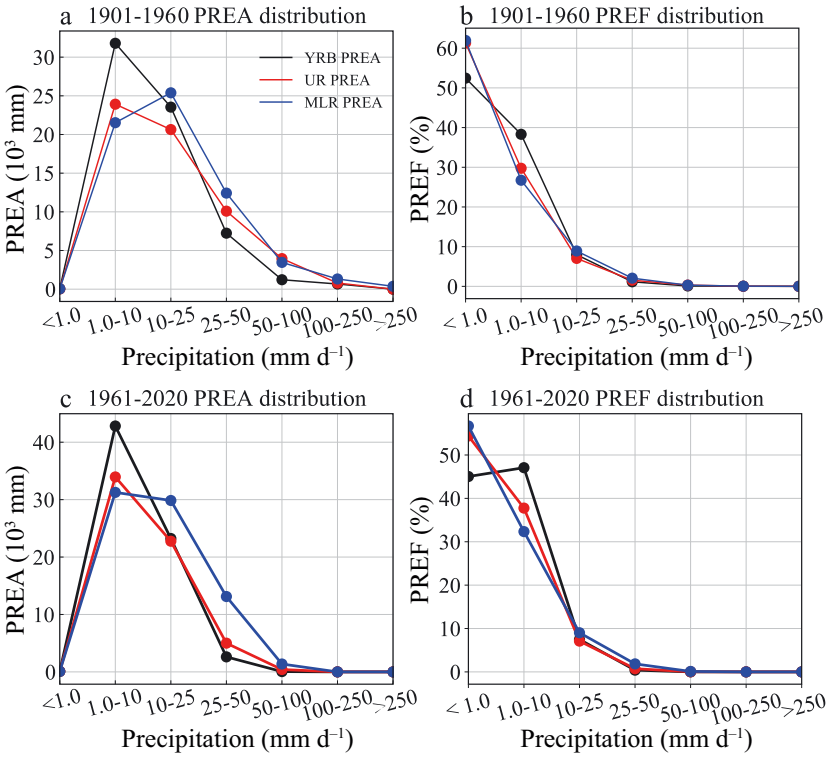

Fig. 4. Daily (a,c) precipitation amount (PREA) and (b,d) precipitation frequency (PREF) distributions over the Yangtze River Basin (YRB), the Upper Reaches (UR), and the Middle and Lower Reaches (MLR) during 1901–1960 and 1961–2020

whereas the stations in the MLR increased significantly in the last 60 yr, with a marked upward trend in the MLR (28.24 mm decade^{-1}) and YRB (17.62 mm decade^{-1}) during 1961–2020 (Fig. 6a). The PRED showed downward trends in the UR and upward trends in the MLR over the 120 yr time series (Fig. 6b). PREI exhibited a remarkable downward trend (approximately −0.16 mm d^{-1} decade^{-1}) prior to 1961 and an upward trend (approximately 0.17 mm d^{-1} decade^{-1}) after 1961 in the YRB, and a remarkable downward trend (approximately −0.34 mm d^{-1} decade^{-1}) before 1961 and an upward trend (approximately 0.23 mm d^{-1} decade^{-1}) after 1961 in the MLR. The UR trend declined significantly during 1901–2020 (Fig. 6c). Overall, the stations in the MLR showed upward trends during 1901–2020, especially in the last 60 yr. In contrast, the stations in the UR showed downward trends during 1901–2020, especially in the first 60 yr.

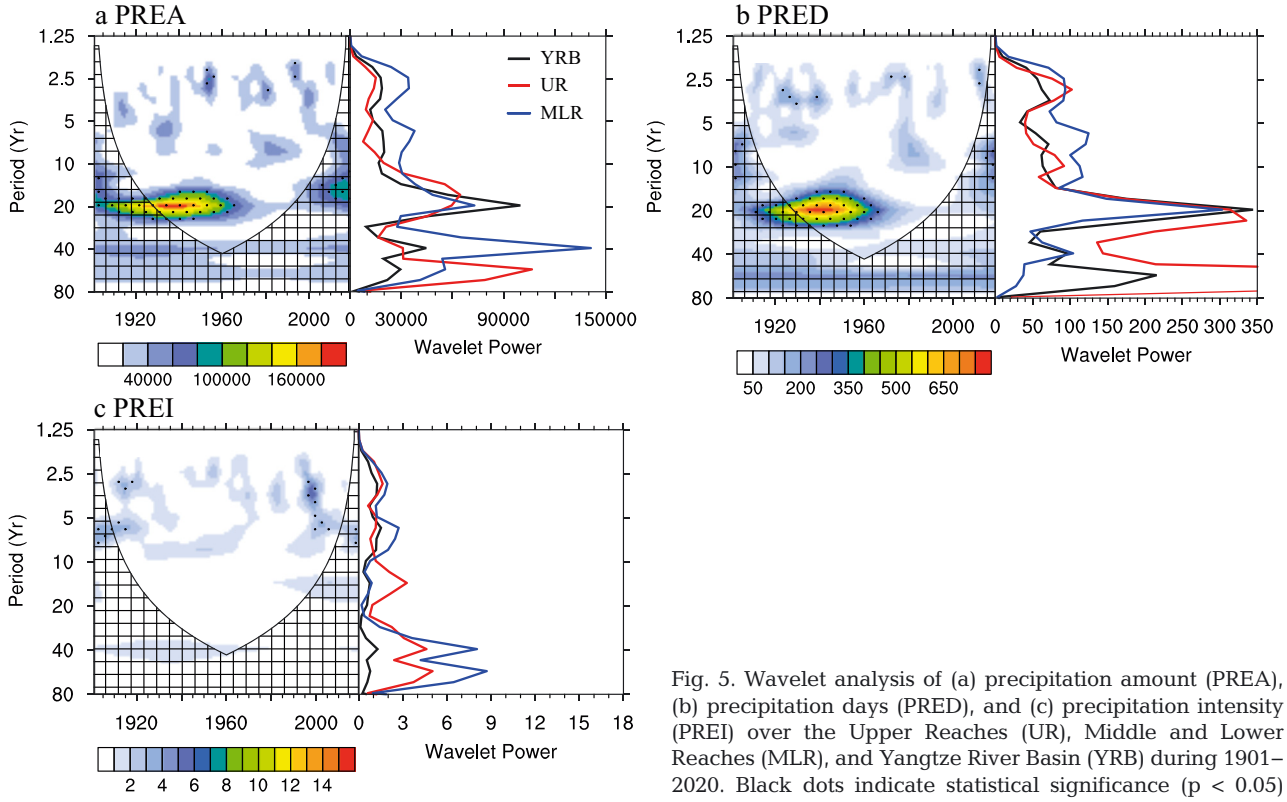

Fig. 5. Wavelet analysis of (a) precipitation amount (PREA), (b) precipitation days (PRED), and (c) precipitation intensity (PREI) over the Upper Reaches (UR), Middle and Lower Reaches (MLR), and Yangtze River Basin (YRB) during 1901–2020. Black dots indicate statistical significance ($p < 0.05$)

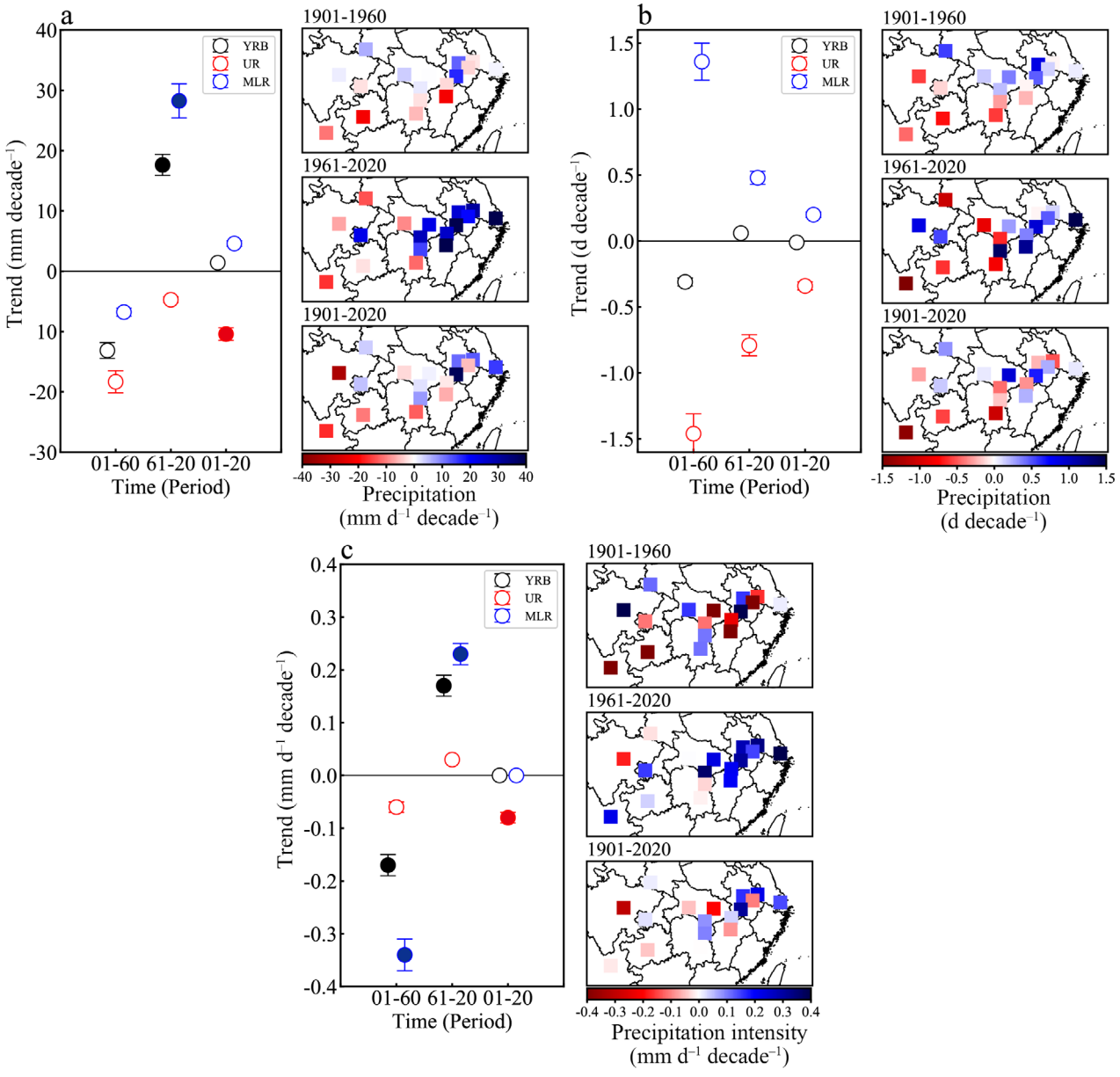

Fig. 6. Dot plots and spatial distributions of linear trends in precipitation values (a) precipitation amount (PREA), (b) precipitation days (PRED), and (c) precipitation intensity (PREI) over the Upper Reaches (UR), Middle and Lower Reaches (MLR), and Yangtze River Basin (YRB) during 1901–2020. Solid circles indicate statistical significance ($p < 0.05$); hollow circles indicate statistical non-significance ($p > 0.05$); error bars represent the standard error of the estimate. Solid blocks in the spatial distribution represent statistical significance ($p < 0.05$). The time range 01–60 represents the period 1901–1960, 61–20 refers to 1961–2020, and 01–20 signifies 1901–2020

3.2. Variability and period of extreme precipitation index

Fig. 7 shows the time series and box plots of anomalies for extreme precipitation indices in the YRB during 1901–2020. The variability of Rx1day and Rx5day was highly consistent, with an obvious peak in the 1910s and a trough in the 1940s (Fig. 7a). Rx1day and Rx5day slightly increased in the early 20th century during the 1900s–1910s, decreased until the 1940s, and then increased again (Fig. 7b). Abnormal values of Rx1day and Rx5day mostly occurred before 1960, with the highest abnormal values occurring in the 1910s. The R20mm and R50mm indices fluctuated, alternating positive and negative values (Fig. 7c). R20mm and R50mm decreased with fluctuation prior to the 1940s and then increased in the last 60 yr. Abnormal values of R20mm and R50mm mostly

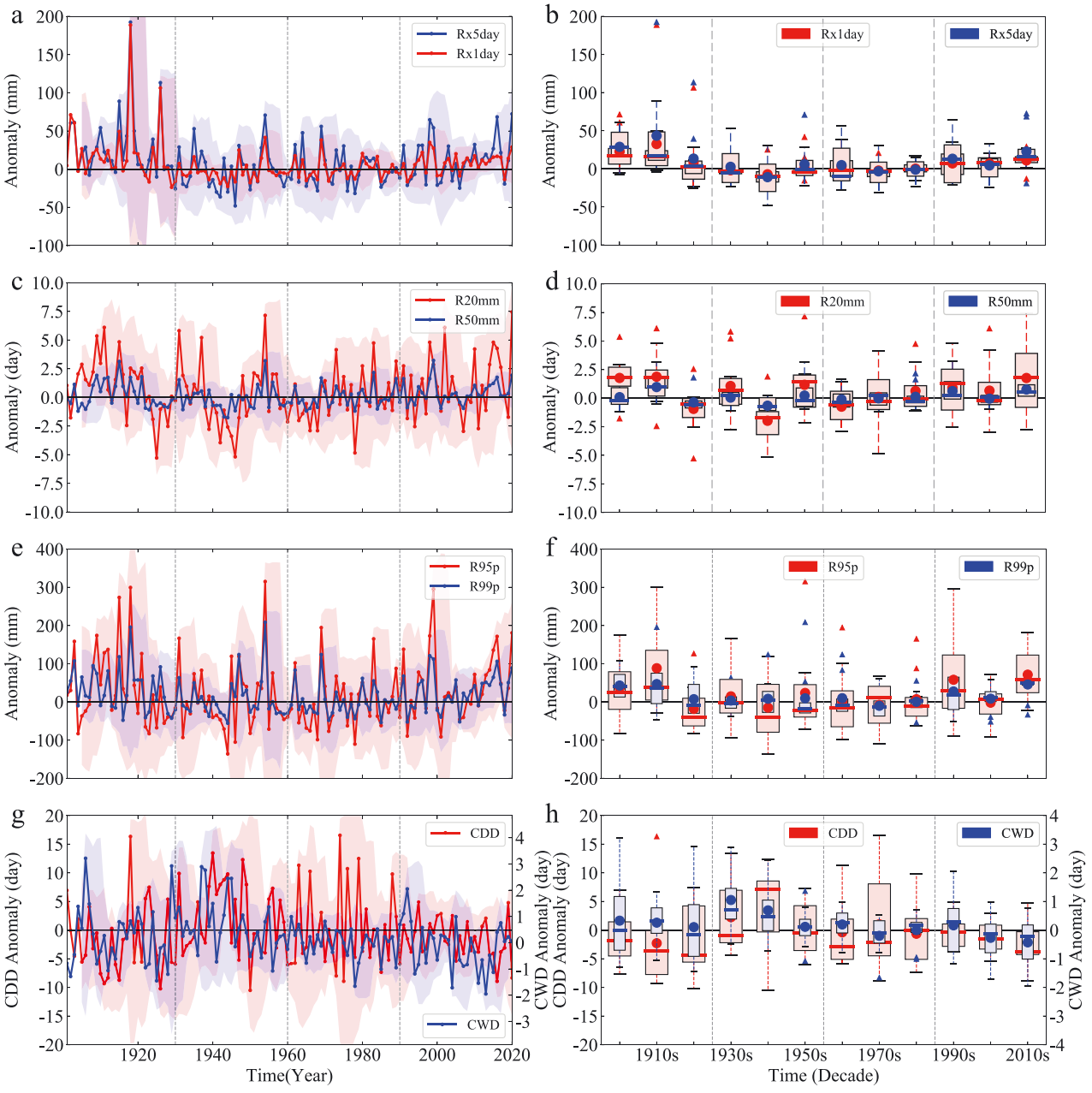

Fig. 7. Time series and box plots of anomalies for the extreme precipitation indices (a,b) maximum 1 d precipitation (Rx1day) and maximum 5 d precipitation (Rx5day), (c,d) heavy precipitation days (R20mm) and rainstorm days (R50mm), (e,f) intense precipitation (R95p) and extreme intense precipitation (R99p), and (g,h) consecutive dry days (CDD) and consecutive wet days (CWD) in the Yangtze River Basin during 1901–2020. Shaded parts represent the range of the 5 yr moving average ± the 5 yr moving SD. The dots, lines, and triangles in box plots represent the average of anomaly, the median of anomaly, and the abnormal values in every decade, respectively

occurred during 1910–1950 (Fig. 7d). The anomalies of R95p and R99p showed positive values that were higher than negative values (Fig. 7e). The highest annual index occurred in 1953, followed by 1918, and the lowest index occurred in 1944. The abnormal values were mostly positive, except for the negative abnormal values in the last 20 yr (Fig. 7f). The CDD and CWD indices increased prior to the 1940s and slightly decreased during 1950–2020, with fluctuations from the 1910s to the 1980s. The highest annual CDD and CWD indices occurred in 1977 and 1907, respectively, followed by 1918 and 1929.

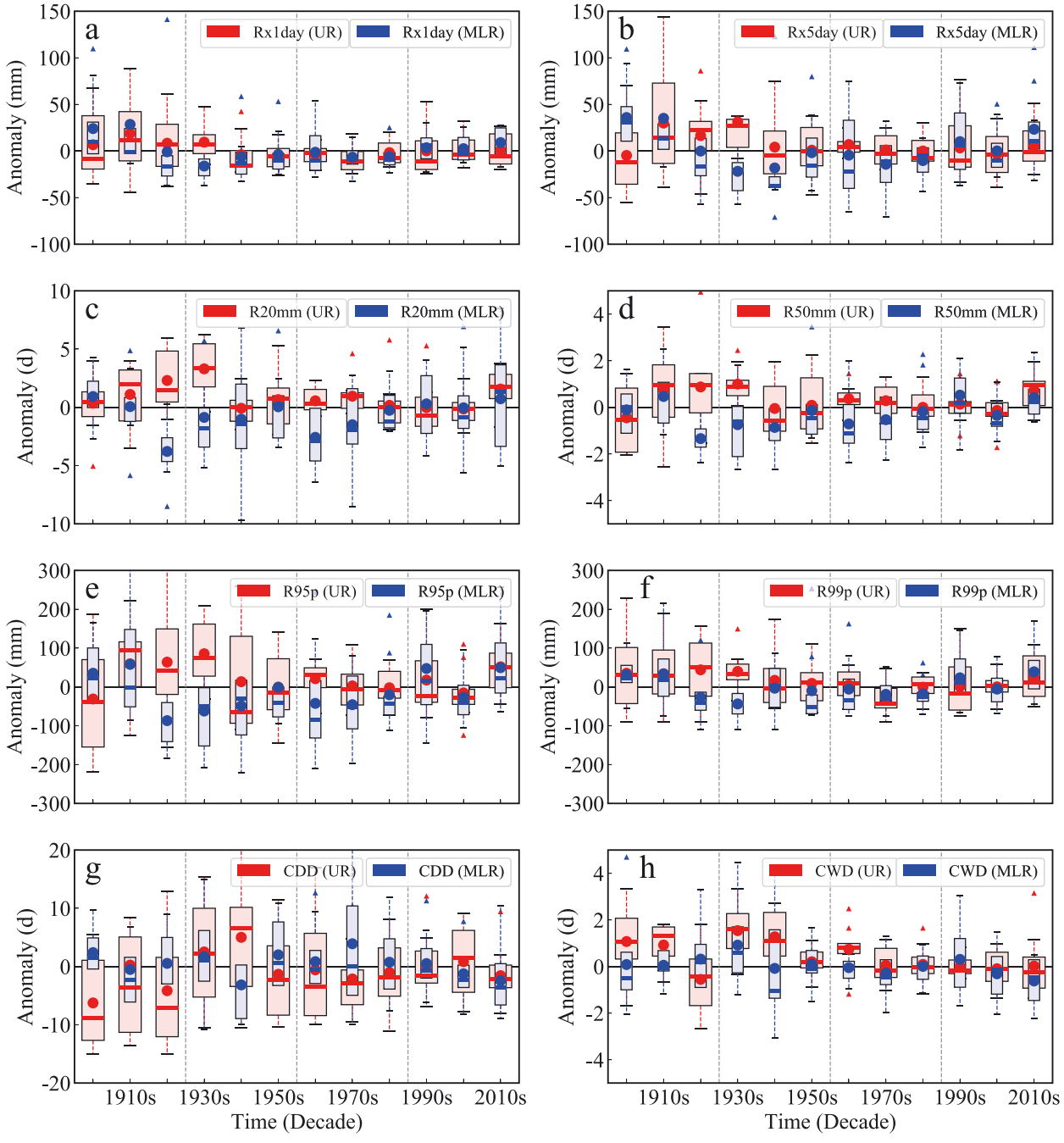

Fig. 8. Box plots of anomalies for the extreme precipitation indices (a) maximum 1 d precipitation (Rx1day), (b) maximum 5 d precipitation (Rx5day), (c) heavy precipitation days (R20mm), (d) rainstorm days (R50mm), (e) intense precipitation (R95p), (f) extreme intense precipitation (R99p), (g) consecutive dry days (CDD), and (h) consecutive wet days (CWD) in the Upper Reaches (UR) and Middle and Lower Reaches (MLR) of the Yangtze River Basin during 1901–2020. Boxplots as in Fig. 2

Fig. 8 shows the box plots of anomalies for extreme precipitation indices in the UR and MLR of the YRB from 1901–2020. The variability of Rx1day in the UR and MLR was generally consistent, except during the early 20th century, from the 1900s–1920s (Fig. 8a). The UR index rapidly increased in the 1900s and decreased in the 1920s, forming an obvious peak in the 1910s, whereas Rx1day in the MLR decreased during the 1900s–1930s and then slightly increased. Although the variability of Rx5day was similar to that

of Rx1day, the abnormal value of Rx5day and inter-annual fluctuations were more dramatic (Fig. 8b). The abnormal values of Rx1day and Rx5day in the YRB are mainly affected by abnormal values in the UR. The R20mm and R50mm indices in the UR fluctuated, alternating positive and negative values. In the MLR, R20mm and R50mm rapidly decreased before 1930 and slightly increased until 2020. The inter-annual fluctuations were more dramatic for R20mm, and the abnormal values were more evident (Fig. 8c,d). The fluctuations in R95p and R99p in the UR were more dramatic than in the MLR. The variabilities of R95p and R99p were similar to that of R20mm (Fig. 8e). The CDD index in the UR and MLR had an obvious peak and trough in the 1940s, respectively. The CWD index in the UR and MLR formed an obvious peak and trough in the 1920s and 1940s, respectively (Fig. 8h).

Fig. 9 shows the periodic characteristics of the extreme precipitation indices in the YRB, UR, and MLR during 1901–2020. The Rx1day and Rx5day indices had 2.5–10 yr significant periodic characteristics in the 1920s, and the wavelet power in the YRB was approximately 1800 (Fig. 9a,b). The powers of Rx1day and Rx5day in the UR (Rx1day: 1500; Rx5day: 2000) and MLR (Rx1day: 2000; Rx5day: 3500) were lower and higher than those in the YRB, respectively. R20mm and R50mm had slight 2.5–5 yr periodic characteristics in the 1910s, 1930s–1950s, and the 1990s (Fig. 9c,d). The significant 20 yr period occurred during 1920–1960. The wavelet power for a 20 yr periodic characteristic of R20mm and R50mm in the YRB was 30 and 5, respectively. The indices in the YRB for the 20 yr period were higher than those in the UR and MLR. Additionally, the MLR indices for the 5 yr period were higher than those for the YRB and UR. The R95p and R99p indices had significant 2.5–5 and 5–10 yr periods in the 1910s and the 1950s, respectively (Fig. 9e,f). The power in the MLR was higher than in the UR and YRB. The CDD had 2.5 yr significant periodic characteristics in the 1970s and 2.5–5 yr slightly periodic characteristics in the 1920s and 1950s. The CWD had 2.5–10 yr significant periodic characteristics in the 1920s–1940s. The CDD and CWD in the UR were higher than those in the MLR and YRB (Fig. 9g,h).

3.3. Trends in the extreme precipitation index

The box plots of linear trends for extreme precipitation indices (Rx1day, Rx5day, R20mm, and R50mm) during 1901–2020 (Fig. 10) show significant upward trends ($p < 0.05$) for Rx1day (2.12 mm decade^{-1}), R20mm (0.34 d decade^{-1}), and R50mm (0.16 d decade^{-1}) during 1961–2020 and significant downward trends ($p < 0.05$) for Rx1day (–2.40 mm decade^{-1}) and Rx5day (–7.94 mm decade^{-1}) during 1901–1960 in the YRB. Fig. 10a,b shows that the trends of Rx1day and Rx5day in the first 60 yr were lower than those in the last 60 yr, which was impacted by the downward trends in the MLR. Although the rates of change of Rx1day and Rx5day in the past 120 yr were non-significant, there were remarkable upward trends in the MLR and downward trends in the UR. The linear trends of R20mm and R50mm were similar to those of Rx1day and Rx5day. However, in both periods of 1901–1960 and 1901–2020, the trends of R20mm were not significant (Fig. 10c,d).

Fig. 11 shows the box plots of the linear trends for the extreme precipitation index (R95p, R99p, CDD, and CWD) during 1901–2020. There were significant upward trends ($p < 0.05$) for R99p (7.28 d decade^{-1}) during 1961–2020 and significant downward trends ($p < 0.05$) for CDD (–0.97 d decade^{-1}) and CWD (0.10 d decade^{-1}) during 1901–1960 and 1901–2020, respectively in the YRB. Fig. 11a,b shows that the average trends for R95p and R99p in the 20th century for the first 60 yr were lower than those in the last 60 yr, which was impacted by the downward trends in the MLR. The linear trends of R95p and R99p were similar to those of the extreme precipitation indices R20mm and R50mm, as shown in Fig. 9. Downward trends were shown for the CDD and CWD for different periods in the 120 yr. Most stations showed a downward trend in the YLB, except for the MLR during 1901–1960 (Fig. 11c,d).

To quantify the trend characteristics of the extreme precipitation index in different regions of the YRB, Fig. 12 shows linear trends for the extreme precipitation index during 1901–1960, 1961–2020, and 1901–2020 in the UR and MLR. From 1901–1960, there were downward trends ($p > 0.05$) for most of the UR and MLR indices. Rx1day and Rx5day showed significant downward trends (–7.93 and –10.53 d decade^{-1}) in the MLR (Fig. 12a). From 1961–2020, most indices showed significant upward trends ($p < 0.05$) in the MLR — except CDD (–0.84 d decade^{-1}) and CWD (–0.08 d decade^{-1}) — and non-significant upward trends ($p > 0.05$) in the UR (Fig. 12b). From 1901–2020, most of the indices showed non-significant trends. The greatest difference in trend for the index was observed for CDD, R95p, and R99p between the UR and MLR (Fig. 12c).

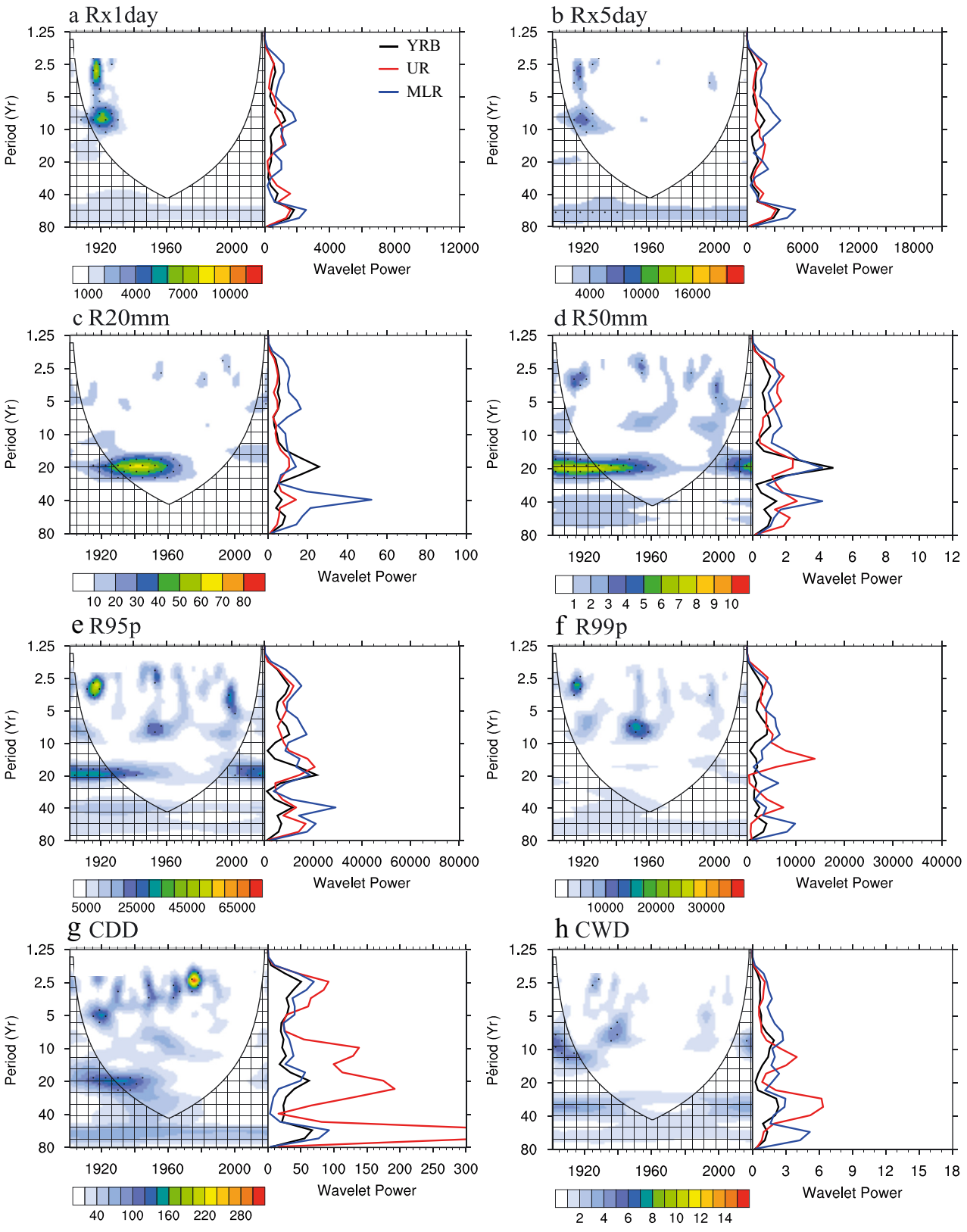

Fig. 9. Wavelet analysis of the extreme precipitation indices (a) maximum 1 d precipitation (Rx1day), (b) maximum 5 d precipitation (Rx5day), (c) heavy precipitation days (R20mm), (d) rainstorm days (R50mm), (e) intense precipitation (R95p), (f) extreme intense precipitation (R99p), (g) consecutive dry days (CDD), and (h) consecutive wet days (CWD) in the Upper Reaches (UR), Middle and Lower Reaches (MLR), and the Yangtze River Basin (YRB) during 1901–2020. Black dots indicate statistical significance ($p < 0.05$)

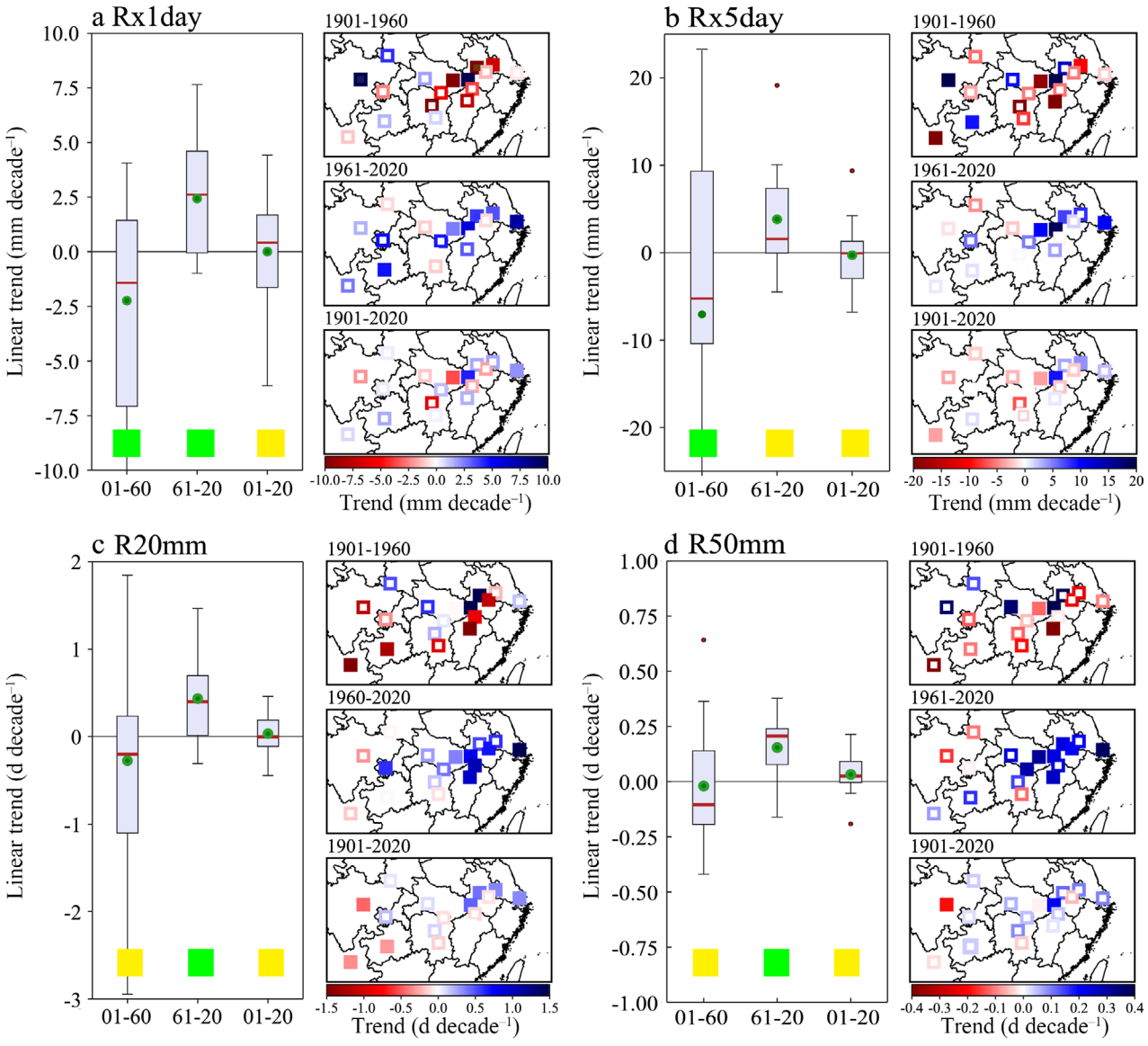

Fig. 10. Box plots and spatial distributions of linear trends for the extreme precipitation indices (a) maximum 1 d precipitation (Rx1day), (b) maximum 5 d precipitation (Rx5day), (c) heavy precipitation days (R20mm), and (d) rainstorm days (R50mm) in the Yangtze River Basin during 1901–1960, 1961–2020, and 1901–2020. Green dots, red lines and small red dots: average of linear trends, median of linear trends and the abnormal values for the 17 stations, respectively; top and bottom of box and whiskers: maximum, minimum, and upper and lower quartiles, respectively; green and yellow squares represent statistical significance ($p < 0.05$) and non-significance ($p > 0.05$), respectively; solid blocks in the spatial distribution represent statistical significance ($p < 0.05$). The range 01–60 represents the period 1901–1960, 61–20 refers to 1961–2020, and 01–20 signifies 1901–2020

4. DISCUSSION

This study examined changes in precipitation values and extreme precipitation indices in the YRB from 1901–2020. The significant findings are that the precipitation values (PREA, PRED, and PREI) and extreme precipitation indices showed substantial fluctuations in the early 20th century and that the linear trends for most values and indices showed a downward trend before 1961 and a significant upward trend after 1961, especially in the MLR.

The conclusion that precipitation and extreme precipitation increased after 1961 is consistent with previous research (Jian et al. 1986, Yang et al. 2005, Huang et al. 2006, Feng et al. 2011, Li et al. 2012, Fu et al. 2013, He et al. 2013, Ren et al. 2015, Zhang et al. 2020) and also, to a certain extent, confirmed the accuracy of the daily precipitation data set in this study. Furthermore, the analysis of the change

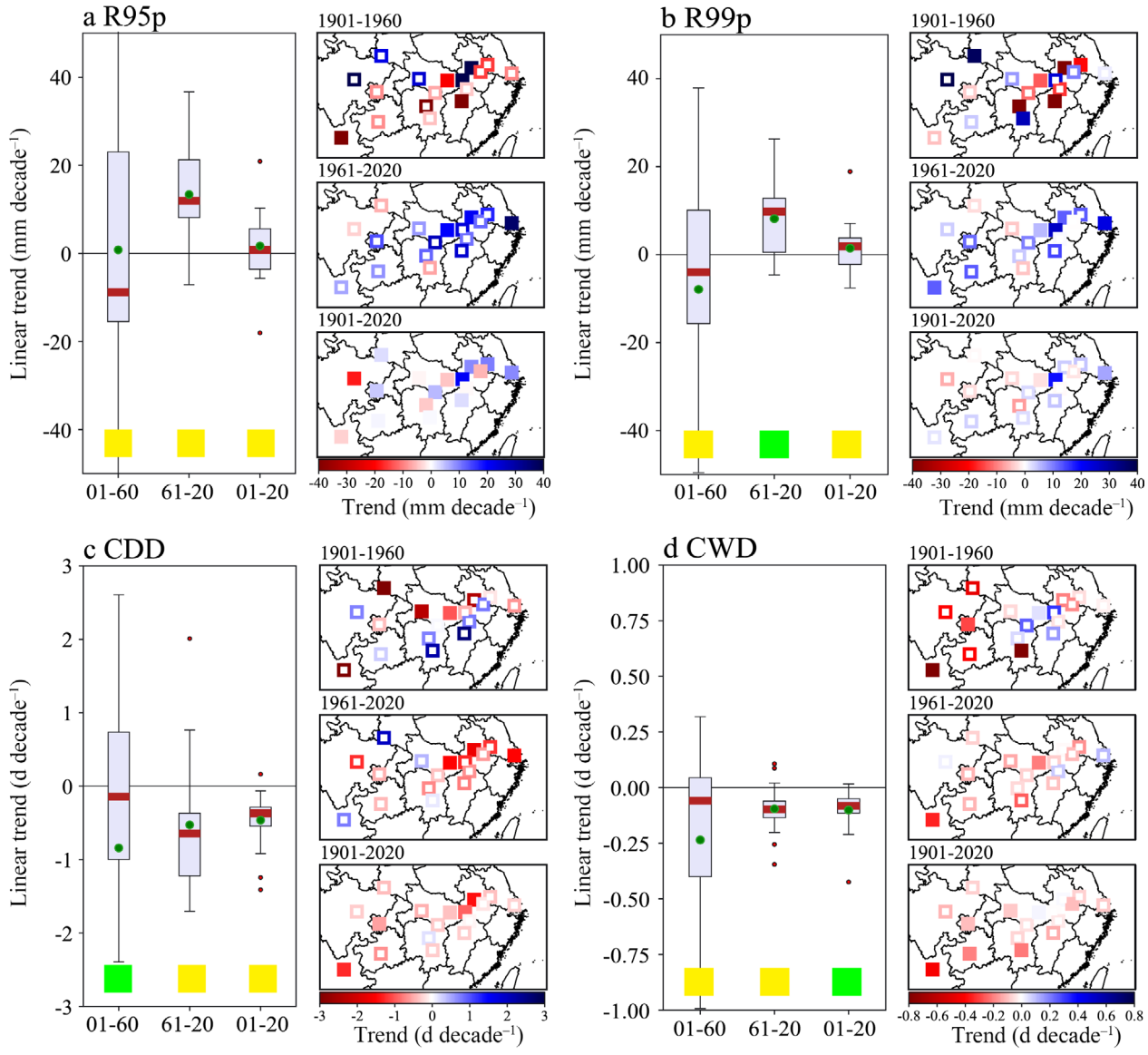

Fig. 11. Box plots and spatial distributions of linear trends for the extreme precipitation indices (a) intense precipitation (R95p), (b) extreme intense precipitation (R99p), (c) consecutive dry days (CDD), and (d) consecutive wet days (CWD) in the Yangtze River Basin during 1901–1960, 1961–2020, and 1901–2020. Green dots, red lines and small red dots: average of linear trends, median of linear trends and the abnormal values for the 17 stations, respectively; top and bottom of box and whiskers: maximum, minimum, and upper and lower quartiles, respectively; green and yellow squares represent statistical significance ($p < 0.05$) and non-significance ($p > 0.05$), respectively; solid blocks in the spatial distribution represent statistical significance ($p < 0.05$). The range 01–60 represents the period 1901–1960, 61–20 refers to 1961–2020, and 01–20 signifies 1901–2020

in extreme precipitation indices makes up for the shortage of research due to the lack of observational data in the first half of the 20th century, which can help us understand the multi-decadal variability in the river basin and, at the same time, provide a reference for verifying the model and reanalysis data.

The extreme precipitation increase in the past 60 yr occurred under the background of global climate warming and rapid urbanization in mainland China. However, in the period of global and regional warming hiatus during 1998–2013, the extreme precipitation events showed a decreasing trend, with R99p (extreme intense precipitation) exhibiting a significant downward trend (Table 3). This implies that changes in global and regional temperature may have an effect on extreme precipitation changes in the YRB. Additionally, the change in regional extreme precipitation is also directly related to the multi-decadal climate variability in East Asia, espe-

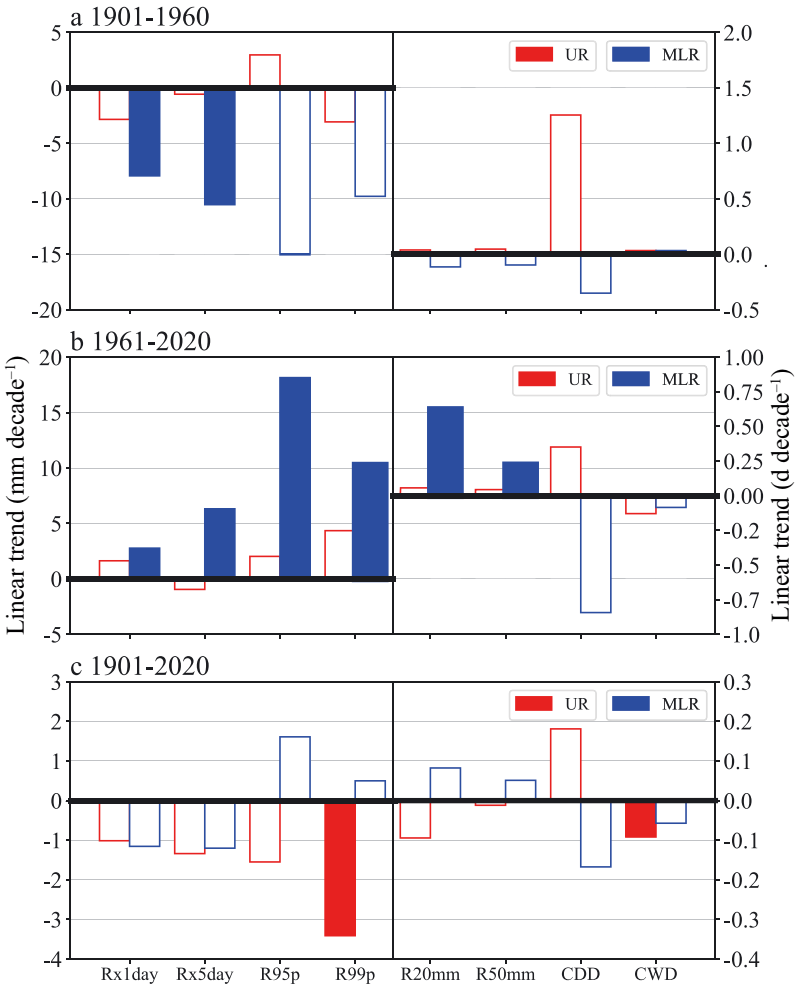

Fig. 12. Linear trends of the extreme precipitation indices maximum 1 d precipitation (Rx1day); maximum 5 d precipitation (Rx5day); intense precipitation (R95p); extreme intense precipitation (R99p); heavy precipitation days (R20mm); rainstorm days (R50mm); consecutive dry days (CDD); and consecutive wet days (CWD) for the Upper Reaches (UR) and the Middle and Lower Reaches (MLR) of the Yangtze River Basin during 1901–1960, 1961–2020, and 1901–2020. Solid bars indicate statistical significance ($p < 0.05$); hollow bars indicate statistical non-significance ($p > 0.05$)

cially to the variability in the East Asian summer monsoon (Ding et al. 2020, Zhou et al. 2022). However, the possible causes of the observed changes in total precipitation and extreme precipitation still require further investigation.

The results reported here contain uncertainties, especially for the period of the early 20th century. First, although the Chinese 60 city daily precipitation data set has undergone strict quality-control and data interpolation for records prior to 1951 (Zhan et al. 2022), compared to the daily precipitation data after 1961, there are obvious differences in the data quality in the early 20th century. The existing record was larger than the effective record prior to 1960, with 17 effective stations after 1960 and only 6 effective stations in 1901. Although the effective number of stations slowly increased until 1937, there was a data-blank period from 1940–1950 (there were no data collected during 1942–1945 in the MLR of the YRB) (Fig. 1, Table 1). Additionally, although the inhomogeneities caused by station relocations and different periods of observation records of individual stations cannot affect regional climate change results, the daily precipitation inhomogeneity of certain stations may lead to uncertainties in the study of station trends during the 20th century (Alexandersson 1986, Liu & Sun 1995, Dai et al. 1997, Wu 2005, Li et al. 2008, Yang & Li 2014). Future studies should further interpolate the early daily precipitation data but also adjust for the inhomogeneities caused by station relocation to establish the city daily precipitation sequence.

Second, studies have demonstrated that the observation records of urban stations contain significant urbanization biases, especially since the mid-20th century in China (Ren et al. 2007, 2008, Ren & Ren 2011, Wang & Ge 2012, Ren & Zhou 2014, Zhang et al. 2019, 2021, 2022, Tysa & Ren 2022). Urbanization can not only cause changes in

Table 3. Linear trends in extreme precipitation indices during 1998–2013 in the Yangtze River Basin. See Table 2 for abbreviation definitions and units. Asterisks indicate statistical significance ($p < 0.05$)

Region	Rx1day	Rx5day	R20mm	R50mm	R95p	R99p	CDD	CWD
YRB	−4.55	−7.76	−2.40	−0.55	−1.25	−0.97*	−59.35	−13.50
UR	−8.65	−8.01	−1.68	−0.06	−2.55	−0.92*	−42.53	−3.75
MLR	−2.32	−7.62	−2.80	−0.82	−0.55	−0.99*	−68.53	−18.81

Table 4. Linear trends for extreme precipitation indices during 1961–2020 at 658 and 17 national weather stations. See Table 2 for abbreviation definitions and units. Asterisks indicate statistical significance ($p < 0.05$)

Stations	Rx1day	Rx5day	R20mm	R50mm	R95p	R99p	CDD	CWD
658 Stations	1.48*	1.75	0.25*	0.10*	10.68*	5.72*	−0.27	−0.12*
17 Stations	2.11*	2.86	0.33*	0.13*	11.28	7.25*	−0.42	−0.10

temperature at urban weather stations through the enhanced urban heat island effect (Ren & Zhou 2014) but also result in changes in radiation, water vapor levels, and cloud cover (Zhang et al. 2022). Studies have shown that the evapotranspiration and PREF in urban areas are smaller than those in rural areas (Varquez & Kanda 2018, Ren et al. 2021, Yang et al. 2021, Zhang et al. 2022); meanwhile, urbanization leads to a reduction in light precipitation and an increase in short-duration intense precipitation at urban stations (Yang et al. 2017, 2021, Tysa & Ren 2022, Yu et al. 2022). Fig. 12 shows a more significant upward trend of intense precipitation over the last 60 yr in MLR than that in the UR. This may have been partially related to the rapid urbanization around the observational sites in central and eastern China over the last half a century. Therefore, the possible influence of urbanization bias on the estimate of extreme precipitation trends in the study region cannot be ignored. It is also necessary to further adjust for urbanization bias in the daily precipitation data in the future.

In this study, we only used 17 city stations to represent changes in extreme precipitation in the YRB. Since 1951, the ground meteorological observation network has gradually been developed in China. In 2020, the National Reference Climate Network and National Basic Meteorological Network in the YRB had 658 observation stations, representing good coverage in terms of temporal and spatial resolution. Table 4 compares the linear trends in the extreme precipitation indices at all 658 stations and the 17 stations in the YRB during 1961–2020. Most of the extreme indices for the 17 stations were higher than those for the 658 stations, except for the CDD. This larger trend may indicate the influence of urbanization on total and extreme precipitation changes and also shows that the trend estimates based on a denser observational network may to some extent reduce the uncertainty in the estimates of extreme precipitation trends in the YRB.

5. CONCLUSIONS

Applying a data set of daily precipitation from 17 stations over the past 120 yr (1901–2020), we analyzed the long-term changes and variabilities in total and extreme precipitation in the YRB. The primary conclusions drawn in this study are as follows:

(1) The precipitation values have slightly increased over the past 120 yr in the YRB, with upward trends in the MLR and downward trends in the UR. Downward and upward trends occurred in the YRB during 1901–1960 and 1961–2020, respectively. The non-precipitation frequency has generally decreased and the light precipitation frequency increased over the last 120 yr.

(2) Most of the extreme precipitation indices showed a decreasing trend in the first 60 yr but reversed after 1961, with slightly upward trends for the whole period of 1901–2020. The trends in extreme precipitation in the UR were lower than those in the MLR during 1901–2020, particularly in the last 60 yr. The upward trends in extreme precipitation in the MLR over the last 60 yr may have been partially related to the influence of rapid urbanization around the observational sites in central and eastern China.

(3) The precipitation and extreme precipitation indices showed clear inter-decadal to multi-decadal and periodic variability. The variability of the most extreme precipitation indices formed a trough in the 1920s and 1940s and a peak in the 1910s, 1950s, and 2010s. There were mainly quasi-periodicals of 5–10 or 20 yr. The upward trend of extreme precipitation may also be a half-cycle feature in the multi-decadal periodic fluctuations.

(4) The observed change in regional extreme precipitation in the MLR of the YRB could be well explained by an urbanization effect around the observational stations and multi-decadal climate variability. These influences may have surpassed the signal from anthropogenic global and regional warming.

Acknowledgements. This study is financed by the National Key Research and Development Program of China (No. 2018YFA0605603, 2020YFA0608203), China Three Gorges Corporation (No. 0704181), and the China Meteorological Administration Youth Innovation Team 'High-Value Climate Change Data Product Development and Application Services (CMA2023QN08).

LITERATURE CITED

Akinsanola AA, Kooperman GJ, Pendergrass AG, Hannah WM, Reed KA (2020) Seasonal representation of extreme precipitation indices over the United States in CMIP6 present-day simulations. Environ Res Lett 15:094003

Alexander LV, Zhang X, Peterson TC, Caesar J and others (2006) Global observed changes in daily climate extremes of temperature and precipitation. J Geophys Res 111: D05109

Alexandersson H (1986) A homogeneity test applied to precipitation data. J Climatol 6:661–675

Bengtsson L, Hagemann S, Hodges KI (2004) Can climate trends be calculated from reanalysis data? J Geophys Res 109:839–856

Chen JM, Lu GH, Wu ZY (2014) Inner-annual distribution characteristics of the extreme precipitation processes events over the Yangtze River Basin. Changjiang Liuyu Ziyuan Yu Huanjing 23:588–594

Chen XC, Xu Y, Xu CH, Yao Y (2014) Assessment of precipitation simulations in China by CMIP5 multi-models. Adv Clim Chang Res 10:217–225 (in Chinese)

Dai A, Fung IY, Del Genio AD (1997) Surface observed global land precipitation variability during 1900–88. J Clim 10: 2943–2962

Ding YH, Liu YJ, Song YF (2020) East Asian summer monsoon moisture transport belt and its impact on heavy rainfalls and floods in China. Shui Kexue Jinzhan 5:629–643 (in Chinese)

Donat MG, Alexander LV, Yang H, Durre I and others (2013) Updated analyses of temperature and precipitation extreme indices since the beginning of the twentieth century: the HadEX2 dataset. J Geophys Res Atmos 118: 2098–2118

Donat MG, Lowry AL, Alexander LV, O'Gorman PA, Maher N (2016) More extreme precipitation in the world's dry and wet regions. Nat Clim Chang 6:508–513

Feng L, Zhou T, Wu B, Li T, Luo JJ (2011) Projection of future precipitation change over China with a high-resolution global atmospheric model. Adv Atmos Sci 28:464–476

Fu G, Yu J, Yu X, Ouyang R and others (2013) Temporal variation of extreme rainfall events in China 1961–2009. J Hydrol (Amst) 487:48–59

Han J, Du H, Wu Z, He HS (2019) Changes in extreme precipitation over dry and wet regions of China during 1961–2014. J Geophys Res D Atmospheres 124:5847–5859

He SQ, Zheng YF, Yin JF (2013) An analysis on precipitation characteristics over middle and lower reaches of Yangtze River in the last 50 years. Shengtai Huanjing Xuebao 22: 1187–1192

Huang RH, Cai RS, Chen JL, Zhou LT (2006) Interdecaldal variations of drought and flooding disasters in China and their association with the East Asian climate system. Chin J Atmos Sci 30:731–741

IPCC (2021) Climate change 2021: the physical science basis. Contribution of Working Group I to the Sixth Assessment Report of the Intergovernmental Panel on Climate Change. Cambridge University Press, Cambridge

Jaffrés JBD (2019) GHCN-daily: a treasure trove of climate data awaiting discovery. Comput Geosci 122:35–44

Jian GM, Mo MH, Zhu S (1986) Precipitation changes and extreme values in the middle and lower reaches of the Yangtze River in the last 100 years. Sci Bull (Beijing) 006: 30–33

Klein Tank AMG, Zwiers FW, Zhang X (2009) Guidelines on analysis of extremes in a changing climate in support of informed decisions for adaptation. Climate Data and Monitoring WCDMP No. 72. World Meteorological Organization, Geneva

Li QX, Jiang ZH, Huang Q, You Y (2008) The experimental mental detecting and adjusting of precipitation data homogeneity in Yangtze data. Yingyong Qixiang Xuebao 19:219–226

Li QX, Peng JD, Shen Y (2012) Development of China homogenized monthly precipitation dataset during 1900–2009. Acta Geogr Sin 67:301–311

Liu XN, Sun AJ (1995) Study on the test method of non-uniformity of annual precipitation series. Qixiang 8:3–6

Min S, Qian YF (2008) Trends in all kinds of precipitation events in China over the past 40 years. Acta Sci Natur Univ Sunyatseni 47:105–110 (in Chinese)

Pan X, Yin YX, Wang XJ (2017) Temporal characteristics and future trend of extreme precipitation in the Yangtze River Basin during 1960 to 2010. Changjiang Liuyu Ziyuan Yu Huanjing 26:436–444

Pendergrass AG, Hartmann DL (2014) Changes in the distribution of rain frequency and intensity in response to global warming. J Clim 27:8372–8383

Ren YY, Ren GY (2011) A remote-sensing method of selecting reference stations for evaluating urbanization effect on surface air temperature trends. J Clim 24:3179–3189

Ren GY, Zhou YQ (2014) Urbanization effect on trends of extreme temperature indices of national stations over mainland China, 1961–2008. J Clim 27:2340–2360

Ren GY, Chu ZY, Chen ZH, Ren YY (2007) Implications of temporal change in urban heat island intensity observed at Beijing and Wuhan stations. Geophys Res Lett 34:89–103

Ren GY, Zhou YQ, Chu ZY, Zhou JG, Zhang AY, Guo J, Liu XF (2008) Urbanization effects on observed surface air temperature trends in North China. J Clim 21:1333–1348

Ren GY, Liu HB, Chu ZY, Zhang L and others (2011) Multi-time-scale climatic variations over Eastern China and implications for the South–North Water Diversion Project. J Hydrometeorol 12:600–617

Ren GY, Ren YY, Zhan YJ, Sun XB, Liu YJ, Chen U, Wang T (2015) Spatial and temporal patterns of precipitation variability over mainland China. II. Recent trends. Adv Water Sci 26:451–465 (in Chinese with English Abstract)

Ren CC, Ren GY, Zhang PF, Tysa SK, Qin Y (2021) Urbanization significantly affects pan-evaporation trends in large river basins of China mainland. Land (Basel) 10:407

Ren ZH, Yu Y, Zou FL, Xu Y (2012) Quality detection of surface historical basic meteorological data. Yingyong Qixiang Xuebao 23:739–747 (in Chinese with English Abstract)

Song F, Zhou T (2014) Inter-annual variability of East Asian summer monsoon simulated by CMIP3 and CMIP5 AGCMs: skill dependence on Indian Ocean–Western Pacific anticyclone teleconnection. J Clim 27:1679–1697

Su DB, Jiang T, Ren GY, Chen ZH (2006) Observed trends of precipitation extremes in the Yangtze River Basin during 1960 to 2004. Adv Clim Chang Res 2:9–14

Tu K, Yan ZW, Dong WJ (2010) Climatic jumps in precipitation and extremes in drying North China during 1954–2006. J Meteorol Soc Jpn 88:29–42

Tysa SK, Ren GY (2022) Observed decrease in light precipitation in part due to urbanization. Sci Rep 12:3864

Varquez ACG, Kanda M (2018) Global urban climatology: a meta-analysis of air temperature trends (1960–2009). NPJ Clim Atmos Sci 1:32

Wang F, Ge QS (2012) Estimation of urbanization bias in observed surface temperature change in China from 1980 to 2009 using satellite land use data. Chin Sci Bull 57:951–958 (in Chinese)

Wang J, Jiang ZH, Yan ML, Zhan JM (2008) Trends of extreme precipitation indices in the mid-lower Yangtze River valley of China during 1960–2005. Sci Meteorol Sin 28:384–388

Wang QX, Li QX, Zhou HN, Wei N, Zing XH, Wu SA (2012) Homogeneity study and comparison analysis on precipitation series over China. Qixiang 38:1390–1398

Wei FY (2007) Modern climate statistical diagnosis and prediction techniques. China Meteorological Press, Beijing, p 99–102

Westra S, Alexander LV, Zwiers FW (2013) Global increasing trends in annual maximum daily precipitation. J Clim 26:3904–3918

Wu ZX (2005) Preliminary analysis of the information on meteorological station historical evolution and its impacts on homogeneity of observational records. Yingyong Qixiang Xuebao 16:461–467

Wu WB, You QL, Wang D (2016) Characteristics of extreme precipitation in China based on homogenized precipitation data. Ziran Ziyuan Xuebao 31:1015–1026

Xu Y, Xu CH (2012) Preliminary assessment of simulations of climate changes over China by CMIP5 multi-models. Atmos Ocean Sci Lett 5:489–494

Yang HQ, Chen ZH, Shi Y, Ren GY (2005) Change trends of heavy rainfall events for last 40 years in the Yangtze Valley. Qixiang 31:66–68

Yang S, Li QX (2014) Improvement in homogeneity analysis method and update of China precipitation data. Adv Clim Chang Res 10:276–281

Yang P, Ren GY, Yan PC (2017) Evidence for strong association of short-duration intense rainfall with urbanization in Beijing urban area. J Clim 30:5851–5870

Yang P, Ren GY, Yan PC, Deng JM (2021) Urbanization reduces frequency of light rain: an example from Beijing City. Theor Appl Climatol 145:763–774

Yu X, Gu X, Kong D, Zhang Q and others (2022) Asymmetrical shift toward less light and more heavy precipitation in an urban agglomeration of East China: intensification by urbanization. Geophys Res Lett 49: e2021GL097046

Zhai PM, Zhang XB, Wan H, Pan XH (2005) Trends in total precipitation and frequency of daily precipitation extremes over China. J Clim 18:1096–1108

Zhai PM, Wang CC, Li W (2007) A review on study of change in precipitation extremes. Adv Clim Chang Res 3:144–148 (in Chinese)

Zhan YJ, Ren GY, Yang S (2018) Change in precipitation over the Asian continent from 1900–2016 based on a new multi-source dataset. Clim Res 76:41–57

Zhan YJ, Chen DH, Liao J, Ju XH, Zhao YF, Ren GY (2022) Construction of a daily precipitation dataset of 60 city stations in China for the period 1901–2019. Clim Change Res 18:670–682

Zhang ML (1993) Precipitation changes in eastern China during the last century. J Atmos Sci 17:451–461

Zhang SQ, Ma ZF (2011) Change tendency and cyclicity analysis of extreme precipitation over Sichuan province during 1961–2009. Ziran Ziyuan Xuebao 26:1918–1929 (in Chinese)

Zhang SQ, Ren GY, Ren YY, Sun XB (2019) Comparison of surface air temperature between observation and reanalysis data over eastern China for the last 100 years. J Meteorol Soc Jpn 97:89–103

Zhang SQ, Ren GY, Ren YY, Zhang YX, Xue XY (2021) A comprehensive evaluation of surface air temperature reanalyses over China against urbanization bias-adjusted observations. Adv Clim Chang Res 12:783–794

Zhang SQ, Ren GY, Ren YY, Tysa SK (2022) Linkage of extreme temperature change with atmospheric and locally anthropogenic factors in China mainland. Atmos Res 277:106307

Zhang X, Alexander L, Hegerl GC, Jones P and others (2011) Indices for monitoring changes in extremes based on daily temperature and precipitation data. Wiley Interdiscip Rev Clim Change 2:851–870

Zhang YX, Ren YY, Ren GY, Wang GF (2020) Precipitation trends over mainland China from 1961–2016 after removal of measurement biases. J Geophys Res D Atmospheres 125:e2019JD031728

Zhao TB, Fu CB, Ke ZJ, Guo WD (2010) Global atmosphere reanalysis datasets: current status and recent advances. Diqiu Kexue Jinzhan 25:242–254

Zhao TB, Wang JH, Dai A (2015) Evaluation of atmospheric precipitable water from reanalysis products using homogenized radiosonde observations over China. J Geophys Res D Atmospheres 120:10703–10727

Zhou C, He Y, Wang K (2018) On the suitability of current atmospheric reanalysis for regional warming studies over China. Atmos Chem Phys 18:8113–8136

Zhou TJ, Zhang WX, Zhang LX, Clark R and others (2022) 2021: a year of unprecedented climate extremes in Eastern Asia, North America, and Europe. Adv Atmos Sci 39: 1598–1607

Editorial responsibility: Oliver Frauenfeld, College Station, Texas, USA
Reviewed by: 3 anonymous referees

Submitted: November 3, 2022
Accepted: March 27, 2023
Proofs received from author(s): June 15, 2023